Optimal Charging of Electric Vehicles for Load Shaping: a Dual Splitting Framework with Explicit Convergence Bounds

Caroline Le Floch, Francois Belletti, Scott Moura

***Abstract*—This paper proposes a tailored distributed optimal charging algorithm for Plug-in Electric Vehicles (PEVs). If controlled properly, large PEV populations can enable high penetration of renewables by balancing loads with intermittent generation. The algorithmic challenges include scalability, computation, uncertainty, and constraints on driver mobility and power system congestion. This article addresses computation and communication challenges via a scalable distributed optimal charging algorithm. Specifically, we exploit the mathematical structure of the aggregated charging problem to distribute the optimization program, using duality theory. Explicit bounds of convergence are derived to guide computational requirements. Two variations of the dual-splitting algorithm are also presented, which enable privacy preserving properties. Constraints on both individual mobility requirements and power system capacity are also incorporated. We demonstrate the proposed dual-splitting framework on a load shaping case study for the so-called California "Duck Curve" with mobility data generated from the Vehicle-to-Grid Simulator.**

***Index Terms*—Communication system operations and management, Distributed Algorithms, Optimization methods, Large-scale systems, Load shedding.**

I. Introduction

PEVs provide a compelling mechanism for demand-side management in the smart grid. Namely, a vehicle-to-grid (V2G) capable PEV can potentially consume, store, and supply energy in a coordinated manner. If properly managed, PEVs can enhance energy infrastructure resilience, enable renewable integration, and reduce economic costs for consumers and energy providers [1]. In addition to these societal-level, infrastructure and environmental benefits, V2G may provide additional revenue streams to PEV owners [2], whose vehicles are parked and un-used 96% of the day [3]. A single PEV can generally consume 5-20 kW, which is insufficient to participate in power grid markets alone. However, populations of PEVs can be aggregated to collectively provide grid services [4]. The main challenge, however, is managing a large population of distributed PEV resources while ensuring (i) computational tractability, (ii) mobility needs, and (iii) power system capacity constraints.

A growing body of literature addresses optimal PEV population charging. This work can be classified into centralized or distributed protocols. Centralized algorithms [5], [6], [7] utilize a central infrastructure to communicate with each agent, collect information, and compute the optimal load profile of the fleet. The challenges for centralized methods are scalability, with respect to communication, computation and privacy.

In distributed optimization algorithms each PEV solves a local problem and communicates information to its neighbors and/or a coordinator [8]. Previous work has studied various aspects of load shaping and PEV smart-charging including filling the night valley of loads (valley filling) in [9], [10], more general driving behaviors in [11], [12], market bidding strategies and market uncertainty in [13], [14], [15] and grid constraints such as transformer overheating [16], [17] and local distribution grid constraints [18], [19], [20]. A wide range of distributed algorithms has been used including game theoretic approaches and Nash Equilibrium in [9], proximal methods in [10], Alternating Direction Method of Multipliers (ADMM) in [11], [12], regret minimization in [21] and stochastic protocols in [22]. The aforementioned methods successfully address various aspects of PEV smart-charging but do not provide precise convergence analysis. In particular, finding the necessary number of iterations to reach a specific precision is crucial to assess implementation burdens for practitioners. In this article, we seek a tailored method for the distributed PEV smart charging problem, and derive computation requirements. We add to existing studies on optimal charging strategies for load shaping as follows:

- We derive a distributed dual-splitting optimization scheme that exploits the unique aggregate charging problem structure (i.e. a summed objective, strong convexity, and independent constraints). We additionally analyze convergence to yield explicit linear rate-of-convergence bounds, providing precise guidance on the relationship between iterations, error and algorithm parameters. To the best of our knowledge, this is the first comprehensive convergence analysis of the coordinated PEV charging problem.
- We propose stochastic variations of the main dual-splitting algorithm. These variations provide communication and computation trade-offs, thus providing options for practitioners.

C. Le Floch is in the Department of Civil and Environmental Engineering in the University of California, Berkeley, 625 Davis Hall, Berkeley, California 94720, USA, (e-mail: caroline.le_floch@berkeley.edu).

F. Belletti is in the Department of Electrical Engineering and Computer Sciences, University of California at Berkeley, USA (e-mail: francois.belletti@berkeley.edu).

S. Moura is an Assistant Professor at the University of California, Berkeley in Civil and Environmental Engineering (e-mail: smoura@berkeley.edu).

*This work was partially supported by the Laboratory Directed Research Development program at Lawrence Berkeley National Laboratory, by the Director, Office of Science, of the U.S. Department of Energy under Contract No. DE-AC02-05CH11231.

As a particular case study of interest we incorporate mobility and power system constraints to quantify demand response opportunities coming from PEVs to shape the California "Duck Curve".

The remainder of the paper is organized as follows. Section II formulates the optimal PEV scheduling problem. Section III derives the distributed optimization algorithm via dual splitting, analyzes convergence, and proposes two alternate algorithm variations. Section IV incorporates grid congestion constraints. Section V provides a case study on load shaping to flatten the "Duck Curve" in California.

TABLE I: Nomenclature

Symbol	Description
N	Number of PEVs
T_h	Time horizon
u_n^t	Charging rate of PEV n at time t
c_n^t	Discharging rate of PEV n at time t due to driving
x_n^t	State Of Charge (SOC) of PEV n at time t
D^t	Net Load at time t (consumption - renewable generation)
B_n	Battery capacity of PEV n
$\overline{P_n^t}$	Maximum charging power of PEV n at time t
$\underline{P_n^t}$	Minimum charging power of PEV n at time t

II. Problem formulation

In this section, we use the notation in Table I and develop an optimization program for synthesizing PEV charging schedules. We use double brackets to denote a discrete set, e.g. $[[1,T_h]] = \{1,2,\cdots,T_h-1,T_h\}$ and we note the vector inner product: $\langle x,y\rangle = x^T y$, for $x,y \in R^n$. We use the vector notations: $u_n = (u_n^1,...,u_n^{T_h}),\ x_n = (x_n^1,...,x_n^{T_h}),\ c_n = (c_n^1,...,c_n^{T_h})$.

A. PEV Charging constraints

Let x_n^t denote the State of Charge (SOC) of vehicle n at time t, u_n^t denotes the charging rate when vehicle n is plugged-in, and c_n^t denotes the driving discharging rate when vehicle n is on road. The battery dynamics are described by a piecewise linear model, with a power conversion efficiency $\eta \leq 1$.

$$x_n^{t+1} = x_n^t + \frac{\eta^m u_n^t}{B_n}\Delta t - \frac{c_n^t}{\eta B_n}\Delta t. \tag{1}$$

$$m = \begin{cases} 1 & \text{if } u_n^t \geq 0, \\ -1 & \text{if } u_n^t < 0, \end{cases} \tag{2}$$

$$x_n^{min} \leq x_n^t \leq x_n^{max} \tag{3}$$

Equations (1), (2) and (3) define a constraint set, which is more binding as η increases, and attains the most binding case when $\eta = 1$ (in practice, $\eta = 1$ models a perfect battery efficiency). Therefore, satisfying the constraints associated with a perfect efficiency ensures that the constraints (1), (2) and (3) are true at every time step $t \in [\![1,T_h]\!]$, for any value of $\eta \leq 1$. For simplicity, and similarly to previous work ([23], [24], [25]), we will use $\eta = 1$ to determine the PEV energy constraints:

$$\frac{B_n}{\Delta t}(x_n^{min} - x_n^{init}) + \sum_{\tau=1}^{t} c_n^\tau \leq \sum_{\tau=1}^{t} u_n^\tau \leq \frac{B_n}{\Delta t}(x_n^{max} - x_n^{init}) + \sum_{\tau=1}^{t} c_n^\tau \tag{4}$$

$$\underline{P_n^t} \leq u_n^t \leq \overline{P_n^t},\ \forall t \in [\![1,T_h]\!] \tag{5}$$

The variable u_n^t can be non zero if and only if PEV n is plugged-in at time t. We denote R_n as the indicator vector

$$R_n^t = \begin{cases} 1, \text{ if EV } n \text{ is plugged in at time } t \\ 0, \text{ otherwise} \end{cases} \tag{6}$$

From this definition, we can derive the equality constraint:

$$(1 - R_n)^T u_n = 0 \tag{7}$$

B. Finite Time Horizon constraints

The above problem has a fixed time horizon T_h. In practice, the lack of a terminal constraint could deplete all the PEVs' energy at the end of the period T_h. For simplicity, we impose that every PEV reaches at least SOC x_n^{final} at the end of the period.

$$\sum_{\tau=1}^{T_h} u_n^\tau \geq \frac{B_n}{\Delta t}(x_n^{final} - x_n^{init}) + \sum_{\tau=1}^{T_h} c_n^\tau \tag{8}$$

This is a conservative constraint, which can be improved in future formulations of the problem.

C. Objective

We denote by D^t the aggregate uncontrollable electric loads combined with the uncontrollable renewable generation. Symbol D^t is the net load and does not include PEV loads [26].

We seek to minimize the variance of net load while preserving battery health. This is formulated by the following optimization program:

$$\min_u \sum_{t=1}^{T_h}(D^t + \sum_{n=1}^{N} u_n^t)^2 + \sigma \sum_{n=1}^{N} ||u_n||^2 \tag{9a}$$

$$\text{st } (1 - R_n)^T u_n = 0 \qquad \forall n \in [\![1,N]\!] \tag{9b}$$

$$\underline{P_n^t} \leq u_n^t \leq \overline{P_n^t} \qquad \forall n \in [\![1,N]\!], \forall t \in [\![1,T_h]\!] \tag{9c}$$

$$(4), (8) \qquad \forall n \in [\![1,N]\!], \forall t \in [\![1,T_h]\!] \tag{9d}$$

The first term $\sum_{t=1}^{T_h}(D^t + \sum_{n=1}^{N} u_n^t)^2$ accounts for the variance of the total load curve. The second term $\sigma \sum_{n=1}^{N} ||u_n||^2$ penalizes the distance from u_n to the zero vector. Therefore σ can be viewed as a battery degradation cost [27]. Battery degradation encompasses a variety of complex mechanisms, which partially depends on charging power magnitude among factors such as temperature, cell chemistry, manufacturing quality, etc. However, for simplicity, we will call this term "degradation cost" in the rest of the paper.

The optimization program is a Quadratic Program (QP) with $T_h \times N$ linear equality constraints and $1 + 4T_h \times N$ linear inequality constraints. For context, consider the Zero Emission Vehicle (ZEV) Action Plan [28] to reach $N = 1.5$ million ZEVs in California by 2025. For $T_h = 24h$ and $\Delta t = 1h$, this yields

a QP with $32M$ variables and $144M$ inequality constraints. Despite the structural simplicity of a QP, the shear problem size requires an untenable amount of memory, thus motivating parallelization methods.

III. Dual decomposition

In this section we develop a dual splitting method and provide a distributed protocol to solve problem (9). Dual splitting strategies are often used to parallelize large scale optimization problems and various methods have been applied to computer vision [29], machine learning [30] or signal processing [31]. Close to the setting under consideration here, the primal-dual approaches developed in [32], [33] deal with block constrained problems. In the following section, we leverage the particular structure of the PEV smart charging problem and develop a novel dual splitting strategy tailored to the average-based input in the objective and the independent constraints. We show that the resultant Gradient Ascent Method assumes updates from every PEV at each time step, and converges to the optimal solution with a linear rate. We later propose two variations based on the Incremental Stochastic Gradient Method (ISGM), which requires updates from only one agent at a time, but converges with a slower rate of convergence.

A. Dual splitting

In the remainder of this paper, we will study the optimization program (9). Let Ω_n denote the feasible set of charging schedules for PEV n given by (9b), (9c), (9d). We define the consensus variable $z^t = D^t + \sum_{n=1}^{N} u_n^t$. Then (9) becomes:

$$\min_{u,z} \quad \sum_{t=1}^{T_h} (z^t)^2 + \sigma \sum_{n=1}^{N} ||u_n||^2 \tag{10a}$$

$$\text{st} \quad z^t = D^t + \sum_{n=1}^{N} u_n^t \tag{10b}$$

$$u_n \in \Omega_n \ \forall n. \tag{10c}$$

The above problem is a quadratic minimization problem with linear constraints, and therefore a convex program. We can dualize the equality constraint (10b) and form the Lagrangian with dual variable λ. Moreover, assume there exists a feasible point u in the convex set formed by constraints (10c) and (10b). Since (10b) is affine and always feasible, (10) is a convex program and admits a feasible point. Slater's condition holds (c.f. [34]) and the strong duality property gives the equivalent problem:

$$\begin{array}{ll} \max\limits_{\lambda^t \in \Re} \min\limits_{u,z} & \sum\limits_{t=1}^{T_h} (z^t)^2 + \sum\limits_{t=1}^{T_h} \lambda^t (z^t - D^t - \sum\limits_{n=1}^{N} u_n^t) + \sigma \sum\limits_{n=1}^{N} ||u_n||^2 \\ \text{st} & u_n \in \Omega_n \ \forall n. \end{array} \tag{11}$$

We first perform the minimization with respect to variable z;

$$\forall t \in [\![1, T_h]\!] \ {z^t}^* = \text{argmin} \ [f_t(z^t) = {z^t}^2 + \lambda^t z^t]$$

$${z^t}^* = -\frac{\lambda^t}{2} \text{ and } f_t({z^t}^*) = -\frac{(\lambda^t)^2}{4}$$

Now, we define $\mu^t = -\lambda^t$ and plug the value of ${z^t}^*$ into (11). Then, the problem is equivalent to:

$$\max_{\mu \in \Re^{T_h}} \frac{-||\mu||^2}{4} + \mu^T D + \sum_{n=1}^{N} \begin{pmatrix} \min\limits_{u_n} & \mu^T u_n + \sigma ||u_n||^2 \\ \text{st} & u_n \in \Omega_n. \end{pmatrix} \tag{12}$$

Note that the contributions of u_n in the objective function (12) are decoupled along $n \in [\![1, N]\!]$. The N minimization subproblems are now independent from each other and can be solved in parallel. In the next sections we will study the Gradient Ascent Method and the Incremental Stochastic Gradient Method to solve this optimization program.

B. Gradient ascent method

Algorithm 1 Gradient ascent

Initialization $\mu = \mu_0$; Choose $\alpha \geq 0$, $\beta \geq 0$
1) Find local optimal solution u_n^k
for n=1 **to** N **do**
Solve $u_n^k = \underset{u_n}{\text{argmin}} \ {\mu^k}^T u_n + \sigma ||u_n||^2$ st $u_n \in \Omega_n$.
end for
2) Update μ
Compute Gradient step $\mu^{k+1} = \mu^k + \frac{\alpha}{k^\beta}(-\frac{\mu^k}{2} + D + \sum u_n^k)$
if Stopping criteria not reached **then**
$k \leftarrow k+1$, Go to **1)**
end if

Algorithm 1 gives the gradient ascent protocol to solve the optimization program with parameters $\alpha \geq 0$, $\beta \geq 0$, such that the gradient ascent step at iteration k is $\frac{\alpha}{k^\beta}$. In this section, we prove that Algorithm 1 converges to the optimal solution and we give complexity bounds. Let $g : \Re^{T_h} \to \Re$ denote the dual objective function:

$$g(\mu) = \frac{-||\mu||^2}{4} + \mu^T D + \sum_{n=1}^{N} \begin{array}{ll} \min\limits_{u_n} & \mu^T u_n + \sigma ||u_n||^2 \\ \text{st} & u_n \in \Omega_n \ \forall n. \end{array}$$

Theorem 1 (Gradient Ascent with constant step-size): The dual problem in Eq (10) has a unique solution μ^* and the gradient ascent with step-size $\alpha = \frac{2\sigma}{\sigma + N}$ converges according to

$$g(\mu^*) - g(\mu_k) \leq \left(\frac{N}{\sigma + N}\right)^k (g(\mu*) - g(\mu_0)) \tag{13}$$

Proof: We will prove Theorem 1 in two steps: (i) show strong concavity of g, then (ii) show that that function g admits Lipschitz gradients.

Step 1: The function $g : \Re^{T_h} \to \Re$ is strongly concave with constant $m = \frac{1}{2}$.

We refer to [34] for generic results about convex functions and for the detailed definition of the strong convexity constant m. Function g is a sum of a strongly concave quadratic function and N functions ψ_n defined by:

$$\psi_n(\mu) = \begin{array}{ll} \min\limits_{u_n} & \mu^T u_n + \sigma ||u_n||^2 \\ \text{st} & u_n \in \Omega_n. \end{array}$$

The set Ω_n is a non-empty convex set. For each μ, $\psi_n(\mu)$ appears as a minimum of a strongly convex function over a convex set, thus it has a unique solution $u_n^*(\mu)$. Let $\tau \in [0,1]$, $\mu_1, \mu_2 \in \Re$.

$$\begin{aligned}
&\tau\psi_n(\mu_1) + (1-\tau)\psi_n(\mu_2) \\
&= \tau \min_{u_n \in \Omega_n} \mu_1^T u_n + \sigma||u_n||^2 + (1-\tau) \min_{u_n \in \Omega_n} \mu_2^T u_n + \sigma||u_n||^2 \\
&\leq \min_{u_n \in \Omega_n} \tau(\mu_1^T u_n + \sigma||u_n||^2) + (1-\tau)(\mu_2^T u_n + \sigma||u_n||^2) \quad (14) \\
&= \psi_n(\tau\mu_1 + (1-\tau)\mu_2)
\end{aligned}$$

Therefore, ψ_n is concave. Now, $g(\mu) = \frac{-||\mu||^2}{4} + \mu^T D + \sum_{n=1}^{N} \psi_n$. The quadratic part is strongly concave with constant $\frac{1}{2}$, therefore g is at least $\frac{1}{2}$ strongly concave.

Step 2: The function $g : \Re^{T_h} \to \Re$ has a Lipschitz continuous gradient with constant $L_g = \frac{1}{2}(1 + \frac{N}{\sigma})$. Since $\psi_n(\mu)$ admits a unique minimum and the function is linear in μ, ψ_n is differentiable and $\nabla\psi_n(\mu) = u_n^*(\mu)$ (see [35]). Using the characterization of minimum of convex functions with $u_n^{*1} = u_n^*(\mu_1)$ and $u_n^{*2} = u_n^*(\mu_2)$, we have:

$$\begin{aligned}
\langle \mu_1 + 2\sigma u_n^{*1}, u_n - u_n^{*1} \rangle \geq 0 \ \forall u_n \in \Omega_n \\
\langle \mu_2 + 2\sigma u_n^{*2}, u_n - u_n^{*2} \rangle \geq 0 \ \forall u_n \in \Omega_n \quad (15)
\end{aligned}$$

Applying these relations respectively to u_n^{*2} and u_n^{*1} we get:

$$\begin{aligned}
\langle \mu_1 + 2\sigma u_n^{*1}, u_n^{*2} - u_n^{*1} \rangle \geq 0 \\
\langle \mu_2 + 2\sigma u_n^{*2}, u_n^{*1} - u_n^{*2} \rangle \geq 0 \quad (16)
\end{aligned}$$

Adding these lines, and using Cauchy Schwarz yields :

$$\begin{aligned}
\langle (\mu_1 - \mu_2) + 2\sigma(u_n^{*1} - u_n^{*2}), u_n^{*2} - u_n^{*1} \rangle \geq 0 \\
\langle (\mu_1 - \mu_2), u_n^{*1} - u_n^{*2} \rangle - 2\sigma||u_n^{*1} - u_n^{*2}||^2 \geq 0 \\
||\mu_1 - \mu_2||||u_n^{*2} - u_n^{*1}|| \geq 2\sigma||u_n^{*1} - u_n^{*2}||^2 \quad (17)
\end{aligned}$$

We conclude that $||u_n^{*1} - u_n^{*2}|| \leq \frac{1}{2\sigma}||\mu_1 - \mu_2||$. Thus, with operations (15), (16) and (17) we can conclude:

$$||\nabla\psi_n(\mu_1) - \nabla\psi_n(\mu_2)|| \leq \frac{1}{2\sigma}||\mu_1 - \mu_2|| \quad \forall n, \ \forall \mu_1, \ \forall \mu_2.$$

Coming back to the definition of function g, we obtain:

$$\begin{aligned}
\nabla g(\mu_1) - \nabla g(\mu_2) &= -\frac{\mu_1 - \mu_2}{2} + \sum_n (u_n^{*1} - u_n^{*2}) \\
||\nabla g(\mu_1) - \nabla g(\mu_2)|| &\leq \frac{\sigma + N}{2\sigma}||\mu_1 - \mu_2|| \quad (18)
\end{aligned}$$

Therefore, g has a Lipschitz continuous gradient with constant $L_g = \frac{\sigma+N}{2\sigma}$.
Now, from [34, Ch. 9, p. 466], the gradient ascent method with stepsize $\frac{1}{L_g}$ converges and gives

$$\begin{aligned}
g(\mu^*) - g(\mu_k) &\leq \left(1 - \frac{m}{L_g}\right)^k (g(\mu*) - g(\mu_0)) \\
&\leq \left(\frac{N}{\sigma + N}\right)^k (g(\mu*) - g(\mu_0)) \quad (19)
\end{aligned}$$

□

Remark 1: Algorithm 1 with constant step-size converges to accuracy ε in $O\big((1 + \frac{N}{\sigma})log(\frac{1}{\varepsilon})\big)$ iterations; the complexity is $O\big((N + \frac{N^2}{\sigma})log(\frac{1}{\varepsilon})\big)$. In other words, the convergence rate is linear with respect to parameter $\frac{\sigma}{N}$ and the complexity is quadratic with respect to N. Hence, it is important to tune the parameter $\frac{\sigma}{N}$ to accelerate the convergence. On the other hand, $\frac{\sigma}{N}$ measures how selfish the agents are: as $\frac{\sigma}{N}$ increases, the penalization for battery degradation increases and the result looses optimality in terms of variance minimization. Fig 1 illustrates this tradeoff for 200 agents. In each case $\mu_0 = D$ where D is the initial load curve. We stop the algorithm when we reach a relative duality gap of 10^{-5}. We note that for $\frac{\sigma}{N} \geq 1$, 10 iterations are enough to reach this precision.

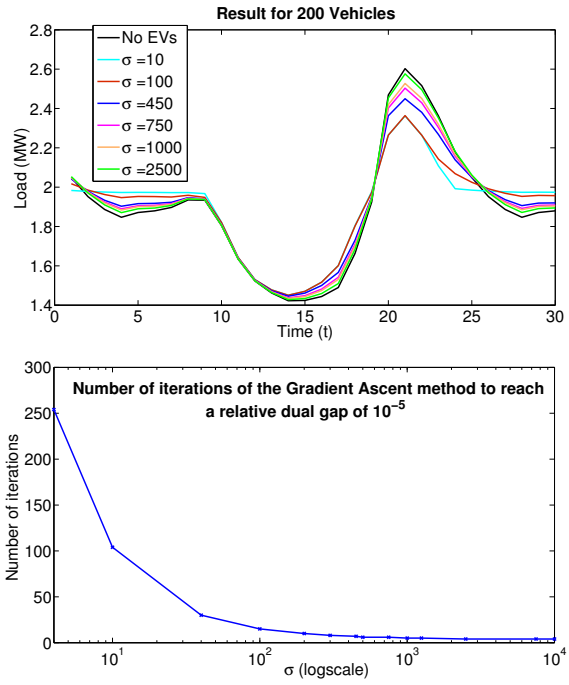

Fig. 1: Impact of σ on convergence rate and results

Remark 2: The derived dual splitting algorithm and Theorem 1 apply for any feasible convex set of constraints Ω_n. Consequently, the algorithm can be adapted to similar problems where each agent has an independent set of convex constraints. This feature is useful for extensions that consider uncertainty via a robust convex set of constraints.

C. Incremental Stochastic Gradient Method

Algorithm 2 Incremental Stochastic Gradient Method

Initialization $\mu = \mu_0$, Choose α, γ, $\beta \geq 0$
1) Find local optimal solution u_i^k
Select i at random in $[\![1, N]\!]$
Solve $u_i^k = \underset{u_i}{\text{argmin}} \ \mu^{kT} u_i + \sigma||u_i||^2$ st $u_i \in \Omega_i$.
2) Update μ
Compute Gradient update step
$\mu^{k+1} = \mu^k + \frac{\alpha}{\gamma + k\beta}(-\frac{\mu^k}{2N} + \frac{D}{N} + u_i^k)$
if Stopping criteria not reached **then**
$k \leftarrow k+1$, Go to **1)**
end if

This section develops a variation of the proposed dual-splitting optimization framework to solve (**??**), called the Incremental Stochastic Gradient Method (ISGM). The stochastic method is an iterative method, which uses unbiased estimates of gradients. This is similar to standard gradient methods in the sense that iterate directions are descent directions only in expectation. We keep the same notations and remark that g can be expressed as:

$$g(\mu) = \frac{1}{N}\sum_{n=1}^{N} \frac{-||\mu||^2}{4} + \mu^T D + N \min_{u_n} \mu^T u_n + \sigma||u_n||^2 \quad \text{st } u_n \in \Omega_n.$$
$$= \frac{1}{N}\sum_{n=1}^{N} g_n(\mu) \tag{20}$$

The incremental gradient method is a version of Stochastic Gradient Method where we pick $i \in [\![1,N]\!]$ uniformly at random, and choose the iterate direction ∇g_i. Note μ^* is the optimum for g and μ_n^* is the optimum for g_n. Convergence of IGSM with constant and decreasing step-size are given by the following two theorems.

Theorem 2 (ISGM with constant step-size): ISGM with constant step-size $\alpha \in [0, \frac{1}{(1+N/\sigma)^2}]$ reaches the ball $B(\mu^*, r)$ with precision ε where $r = \frac{1}{1+2\alpha L_g^2}\frac{2\alpha}{N}L_g^3 \sum_{i=1}^{N} ||\mu_i^* - \mu^*||^2$ in $\frac{1}{\alpha(1-2\alpha L_g^2)}\ln(\frac{||\mu_0-\mu^*||}{\varepsilon})$ iterations.

Theorem 3 (ISGM with decreasing step-size): ISGM with decreasing step-size $\alpha_k = \frac{1}{(1+N/\sigma)^2+k}$ converges to the optimal solution μ^* and

$$\mathbb{E}(g(\mu^*) - g(\mu_k)) \leq \frac{1}{N}\sum_{i=1}^{N} ||\mu_i^* - \mu^*||^2 \frac{1}{(1+N/\sigma)^2+k} \tag{21}$$

Proof of Theorems: We prove Theorem 2 and 3 by showing that we can find L and B such that $\mathbb{E}\big(||\nabla g(\mu)||^2\big) \leq L^2||\mu - \mu^*||^2 + B^2$.

Step 1: The function $g_n : \Re^{T_h} \to \Re$ has a Lipschitz continuous gradient with constant $L_n = L_g = \frac{1}{2}(1+\frac{N}{\sigma})$. This is shown by following the same procedure as Step 2 of Theorem 1 proof.

Step 2: Show $\mathbb{E}\big(||\nabla g_i(\mu)||^2\big) \leq 2L_g^2||\mu - \mu^*||^2 + B^2$ with $L_g = \frac{1}{2}(1+\frac{N}{\sigma})$ and $B^2 = \frac{1}{2N}(1+\frac{N}{\sigma})^2 \sum_{i=1}^{N} ||\mu_i^* - \mu^*||^2$. Using the Cauchy Schwarz inequality and the Lipschitz condition, we obtain:

$$\begin{aligned}
\mathbb{E}\big(||\nabla g_i(\mu)||^2\big) &\leq \mathbb{E}\big(L_i^2||\mu - \mu_i^*||^2\big) \\
&\leq \mathbb{E}\big(2L_i^2||\mu - \mu^*||^2 + 2L_i^2||\mu_i^* - \mu^*||^2\big) \\
&= \frac{2}{N}\sum_{i=1}^{N} L_g^2||\mu - \mu^*||^2 + \frac{2}{N}\sum_{i=1}^{N} L_g^2||\mu_i^* - \mu^*||^2 \\
&= 2L_g^2||\mu - \mu^*||^2 + B^2
\end{aligned} \tag{22}$$

This is the condition $\mathbb{E}\big(||\nabla g(\mu)||^2\big) \leq L^2||\mu - \mu^*||^2 + B^2$. With these particular values of L and B, results in [36] can be used to establish the step-sizes and convergence rates of Theorem 2 and 3. □

Remark 3: Similarly to Remark 1, Theorem 2 and Theorem 3 show that the computation time depends only on the parameter $\frac{\sigma}{N}$. Parameter $\frac{\sigma}{N}$ measures the tradeoff between the regularity of the objective function (convergence speed) and the optimality of the solution (load shaping performance). In particular, when $\frac{\sigma}{N}$ increases, the number of necessary iterations decreases but the optimal solution becomes less optimal in terms of load shaping.

D. Comparison of algorithms

This sections shows computation and communication tradeoffs between the algorithms.

1) Convergence speed: Theorem 2 states that the convergence rate of Algorithm 2 with constant step size is linear, similar to Algorithm 1. Theorem 3 states that the convergence rate of Algorithm 2 with decreasing step size is $\frac{1}{k}$, which is much slower than Algorithm 1. Note that an Incremental Method iteration is N times faster than a Gradient Ascent iteration. Thus, the convergence speed of Algorithm 2 with constant step-size is usually faster, but converges only to a certain precision r. Algorithm 2 should be used when the aggregator needs a fast convergence and is satisfied with an approximate solution.

2) Privacy: In the stochastic configuration, only one random PEV needs to communicate with the aggregator at each time step. This significantly reduces the required communication between each PEV and the aggregator, thus increasing resistance to hacking attacks and improving cyber-security [37]. Consequently, Algorithm 2 with decreasing step-size should be used when the aggregator is concerned about privacy.

Figure 2 and 3 show the values of the primal and dual objectives for each of the three methods. We stop Algorithm 1 and 2 when the number of iteration exceeds 2×10^5, or the relative duality gap reaches 10^{-3}; N_{it} denotes the number of necessary iterations to converge to the desired precision $\varepsilon = 10^{-3}$. For each case, we choose the starting point $\mu_0 = D$ where D is the load curve ("Duck Curve"). This shows that all the algorithms converge faster as the parameter $\frac{\sigma}{N}$ increases. For $\sigma = 200$, Algorithm 1 and Algorithm 2 with constant step-size converge to the required precision:

- Algorithm 1 needs 5 full-gradient iterations.
- Algorithm 2 needs 6193 stochastic iterations, which corresponds to $\frac{6193}{200} \simeq 31$ full-gradient iterations.

IV. Power network capacity constraints

In this section we adapt the above methodology to include grid capacity constraints, as studied in [16], [17].

A. Integration of congestion constraints

The algorithms from Section III are likely to create scenarios where most vehicles charge during low net-load hours, and discharge during high net-load hours. This coordination pattern may provoke power congestion and reverse power flows on

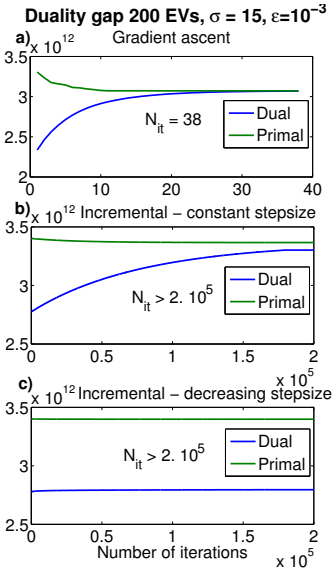

Fig. 2: Duality gap $\sigma = 15$

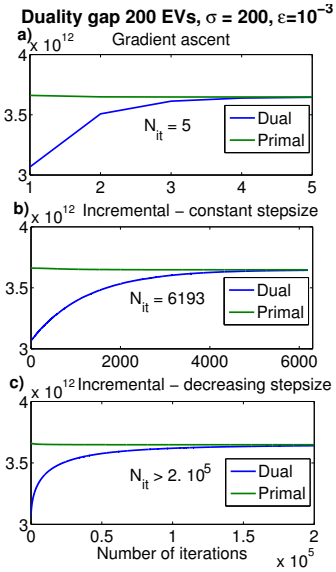

Fig. 3: Duality gap $\sigma = 200$

distribution lines. In particular, distribution system substations may become overloaded and induce equipment failure and large power outages [38], [39]. We consider preventing these dangerous side effects by setting active power capacity constraints for each feeder.

We consider a network with S feeders and denote by $\mathbb{S}_d$ the set of agents that are connected to the feeder d. The aggregator constrains the aggregated PEV power as follows:

$$L_d^t \leq \sum_{j \in \mathbb{S}_d} u_j^t \leq M_d^t \;\; \forall d \in [\![1,S]\!], t \in [\![1,T_h]\!]. \tag{23}$$

where M_d^t and L_d^t denote the remaining capacity of $\mathbb{S}_d$ at time t and can be determined by forecasting the net load connected to $\mathbb{S}_d$ at time t (without PEVs). In this paper we do not model the impact of PEVs at the distribution network bus level, instead we assume an independent system operator or utility provides constraints for the aggregated PEV power at the feeder level and ensures grid reliability. The optimization problem with congestion constraints is:

$$\min_u \sum_{t=1}^{T_h} (D^t + \sum_{n=1}^{N} u_n^t)^2 + \sigma \sum_{n=1}^{N} ||u_n||^2 \tag{24a}$$

$$\text{st } \forall n \in [\![1,N]\!], u_n \in \Omega_n \tag{24b}$$

$$\forall d \in [\![1,S]\!], L_d \leq \sum_{j \in \mathbb{S}_d} u_j \leq M_d \tag{24c}$$

We define the same consensus variable $z^t = D^t + \sum_{n=1}^{N} u_n^t$, and the conclusions from equations (11), (**??**) still hold. Then, the distributed problem becomes:

$$\max_{\mu \in \Re^{T_h}} \frac{-||\mu||^2}{4} + \mu^T D \quad + \quad \sum_{d=1}^{S} \sum_{n \in S_d} \min_{u_n} \mu^T u_n + \sigma ||u_n||^2 \tag{25}$$

$$\text{st} \quad \forall n \in [\![1,N]\!], u_n \in \Omega_n$$

$$\forall d \in [\![1,S]\!], L_d \leq \sum_{j \in S_d} u_j \leq M_d$$

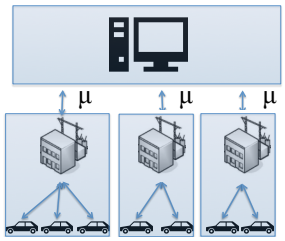

Fig. 4: Semi distributed

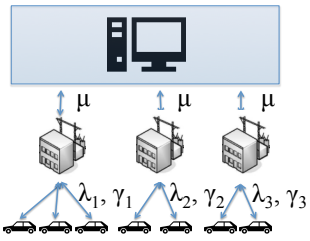

Fig. 5: Fully distributed

We can further dualize the congestion constraints with dual variables λ_d, γ_d to obtain:

$$\max_{\substack{\mu \in \Re^{T_h} \\ \lambda_d, \gamma_d \in \Re^{+T_h}}} \frac{-||\mu||^2}{4} + \mu^T D + \sum_{d=1}^{S} \sum_{n \in S_d} \min_{u_n} \mu^T u_n + \sigma ||u_n||^2 \tag{26}$$

$$+ \lambda_d^T (u_n - M_d) + \gamma_d^T (L_d - u_n)$$

$$\text{st } \forall n \in [\![1,N]\!], u_n \in \Omega_n$$

Equations (25) and (26) show two ways to solve the optimization program with congestion:

- In (25), the problem is semi-distributed (see fig 4). Each subsystem S_d is associated with a Quadratic Program of size $T_h \times N_d$ where N_d is the number of vehicles in S_d. Thus, the complexity of each Quadratic Program scales as $O(T_h^3 \times N_d^3)$. All the results from Section III still hold, where N agents are replaced by S subsystems. This formulation is not scalable, but may be computationally tractable if the size of each subsystem is small.
- In (26), the introduction of dual variables λ_d and γ_d enables a fully distributed system (see fig 5). The triplet of dual variables (μ, λ, γ) is comprised of the global price μ and the congestion prices (λ_d, γ_d).

B. Distributed optimization under congestion constraints

In this subsection we study formulation (26) in more detail. Algorithm 3 proposes an accelerated projected gradient ascent to solve (26). Let y denote the full dual variable $[\mu, \lambda, \gamma]$, the dual objective $f : (\mathbf{R} \times \mathbf{R}^+ \times \mathbf{R}^+) \to \mathbf{R}$ is:

$$f(y) = \frac{-||\mu||^2}{4} + \mu^T D \tag{27}$$

$$+ \sum_{d=1}^{S} N_d (\gamma_d^T L_d - \lambda_d^T M_d) \sum_{d=1}^{S} \sum_{n \in S_d} \min_{u_n} (\mu^T + \lambda_d^T - \gamma_d^T) u_n + \sigma ||u_n||^2$$

$$\text{st } \forall n \in [\![1,N]\!], u_n \in \Omega_n$$

Let Pr denote the projection on the set $(\mathbf{R} \times \mathbf{R}^+ \times \mathbf{R}^+)$. We can find the optimal solution of (26) with a projected gradient ascent. Algorithm 3 presents an accelerated projected gradient ascent using Nesterov iterations [40].

Theorem 4 (Accelerated Projected Gradient Method): The accelerated projected gradient ascent in Algorithm 3 with step-size $\alpha = \frac{2\sigma}{\sigma + N}$ converges to an optimal solution y^* with

$$f(y^*) - f(y_k) \leq \frac{2(\sigma + N)}{\sigma (k+2)^2} ||y^* - y_0||$$

Algorithm 3 Accelerated Projected Gradient Method

Initialization y_0, y_1, $\theta_0 = 1$, Choose α
1) Find local optimal solution u_n^k
for d=1 **to** S **do**
  for n=1 **to** N_d **do**
    Solve Local Quadratic Program $QP_n(\mu^k, \lambda^k, \gamma^k)$
    $u_n^k = \underset{u_n}{\text{argmin}} \ (\mu^k + \lambda_d^k - \gamma_d^k)^T u_n + \sigma||u_n||^2$ st $u_n \in \Omega_n$
  end for
end for
2) Compute β_k
$\theta_k = \frac{1}{2}(-\theta_{k-1}^2 + \sqrt{\theta_{k-1}^4 + 4\theta_{k-1}^2})$
$\beta_k = \theta_k(\frac{1}{\theta_{k-1}} - 1)$
3) Nesterov Gradient update step $y = (\mu, \lambda, \gamma)$
$z_k = y_k + \beta_k(y_k - y_{k-1})$
$y_{k+1} = y_k + \alpha \ \Pr(\Delta f(z_k))$
if Stopping criteria not reached **then**
  $k \leftarrow k+1$, Go to **1)**
end if

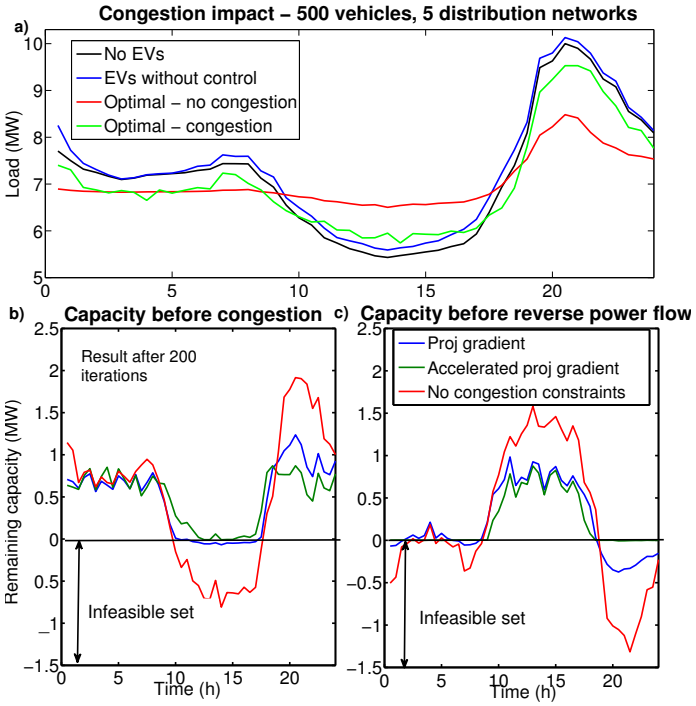

Fig. 6: Impact of congestion constraints

Proof: Note that f is weakly concave and has Lipschitz continuous gradients with constant $L_g = \frac{\sigma+N}{2\sigma}$ (see proof of Theorem 1 for details). Reference [40] gives the corresponding convergence rate for the accelerated Nesterov method.

Figure 6 shows the result for 500 EVs and 5 distribution subsystems with and without congestion constraints. For the 5 subsystems we simulate congestion constraints, which are proportional to the number of PEVs and charger power rate, such that all PEVs cannot be charging or discharging at the same time.Figure 6 shows that the congestion constraints limit the charging and discharging flexibility of the aggregator, especially during the peaks of underconsumption (2pm) and overconsumption (9pm).

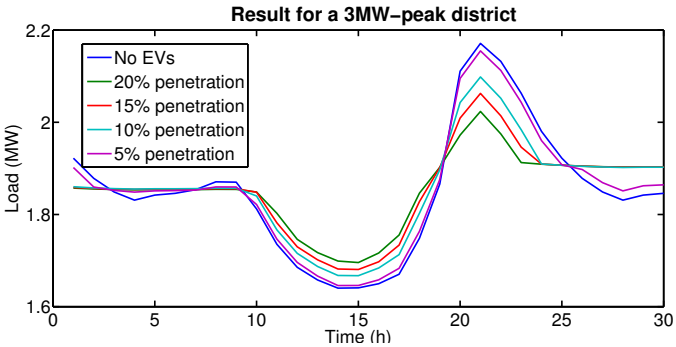

Fig. 7: Impact of PEV penetration on Demand Response

Remark 4: A simple projected gradient ascent could be performed to find the optimal solution of problem (26). However, Theorem 4 states that the number of iterations to reach precision ε scales as $\frac{1}{\sqrt{\varepsilon}}$ for the accelerated method, as compared to $\frac{1}{\varepsilon}$ for a simple projected gradient ascent. Figure 6 b) and 6 c) show the distance from the feasible set after 200 iterations for both the accelerated and standard projection methods. In these two plots the feasible set is the half plan of positive Remaining Capacity values. This shows that 200 iterations are sufficient to approach feasibility with the accelerated method but not with the standard method.

V. Results, Application to the Duck Curve

In this section we apply the proposed dual splitting algorithm to flatten the California "Duck Curve" via managed PEV charging. In this section, we do not consider capacity constraints. The Vehicle-to-Grid Simulator (V2G-Sim), developed at Lawrence Berkeley National Laboratory [41], is used to model the driving and charging behavior of individual PEVs. V2G-Sim is an agent-based simulator that incorporates mobility data from the 2009 National Household Travel Survey (NHTS) [42]. Reference [43] provides more details about the V2G-Sim modeling methodology.

A. Impact of PEV penetration on Demand Response

In this section, we fix the scale $\frac{\text{Number of cars}}{\text{Maximum Peak Load}}$. We assume that the total peak load in California is 26000 MW and the total number of cars in California is 13.3×10^6. This ratio is kept constant to simulate areas of different size and study the impact of PEV penetration in California. Figure 7 shows the impact of PEV penetration on a 3MW peak area, which approximately corresponds to 1600 cars. We consider the only available charging infrastructure is Level 1 chargers at home. It is interesting to see that 20% penetration (315 PEVs) suffices to reduce the evening ramp by a factor of 2.

B. Comparison with other algorithms

In this section, we compare the load shaping performance of the proposed distributed algorithm against decentralized strategies, such as exogeneous marginal pricing and Time

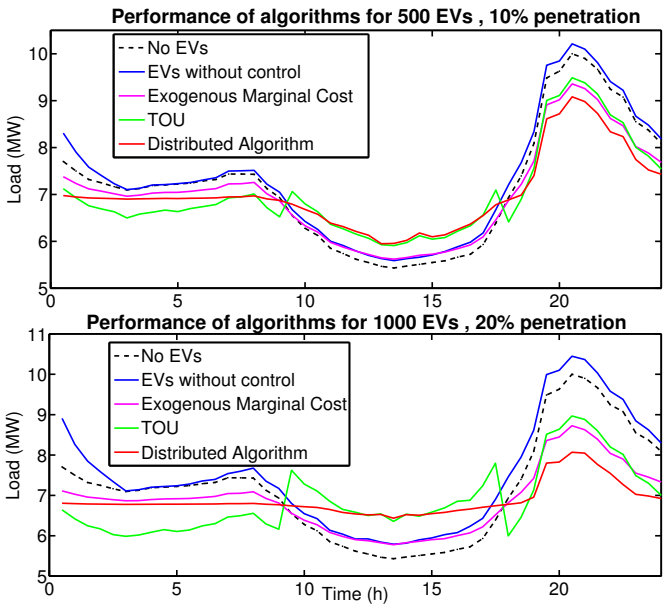

Fig. 8: Comparison of various pricing methods

Of Use (TOU) pricing ([9], [44]). We seek to assess the performance with respect to the demand response impact. As such, other distributed methods are not considered, since they would yield the same load shaping result, although may require different numbers of iteration.

- *Exogenous Marginal Price*: In this scenario, we consider a fixed pricing signal $\mu^t = \frac{\sigma 10^4}{Cap} D^t$, where Cap is the maximum Load capacity from loads and PEVs, and D is the Net Load without PEVs. This price signal is synthesized by multiplying the net load signal D by scaling factor $\frac{\sigma 10^4}{Cap}$. Thus, this method naturally assigns high prices to peak consumption times, and low prices when total net load is low. This concept is explored in [9] for example.
- *TOU Price*: This pricing method is based on off-peak, partial peak and peak periods. It has been used by several utilities to regulate the demand (see *PG&E* for example [44]). In this scenario we divide the 24h period into 3 groups and assign the corresponding *PG&E* rates for off-peak, partial-peak, and peak periods.

Figure 8 shows the effect of the 3 price signals in two different penetration scenarios. In general, the three methods tend to flatten the net load curve, however TOU and Exogenous prices are suboptimal. Figure 8 b) shows that TOU pricing yields non-flat load for a large penetration of PEVs. Because we assume that all the agents are price takers, the transitions between partial-peak and off-peak periods (9am and 6pm) create large undesirable ramping. That is, all the PEVs start charging at 9am and stop at 6pm.
This example shows that exogenous methods can be counterproductive in certain scenarios. It is preferable to have a systematic, model-based method to determine price signals.

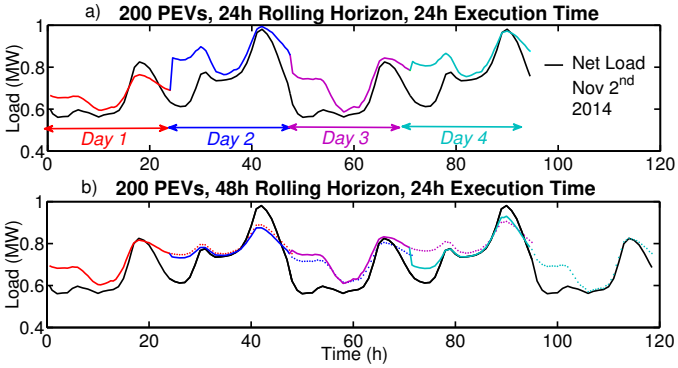

Fig. 9: Rolling horizon implementation: the colored lines represent the load shape after PEV smart charging, full lines are real implementation and dashed lines planned implementation

C. Load continuity and real implementation

Equation 9 is a finite time horizon optimization program. In practice, this method could create discontinuities (ramping) between two separate time periods. This is critical in the context of load shaping since we aim to flatten a continuous energy curve. This point can be handled with rolling horizon techniques. Let T_r define the Rolling Horizon and T_e the execution horizon, we augment the objective function (9a) with additional costs due to time steps $t \in [\![T_e, T_r]\!]$ but implement the given solution only for time steps in $[\![1, T_e]\!]$:

$$\min_u \sum_{t=1}^{T_e} (D^t + \sum_{n=1}^{N} u_n^t)^2 + \sum_{t=T_e+1}^{T_r} (D^t + \sum_{n=1}^{N} u_n^t)^2 + \sigma \sum_{n=1}^{N} ||u_n||^2 \tag{28}$$

Figure 9 shows a four day implementation. Figure 9 a) shows the case where $T_e = T_r = 24$h and Figure 9 b) shows the case where $T_e = 24$h and $T_r = 48$h. In Figure 9 b) there are no discontinuities between two distinct execution periods (full lines), whereas figure a) shows some high power ramping between two different days (particularly between Day 1 and Day 2). The plot illustrates that this implementation method ensures load continuity between different execution periods.

VI. Conclusion

This article studies distributed optimal charging algorithms for PEV charging via dual splitting. We define a global optimization problem, which seeks to coordinate PEV charging/discharging to minimize the load variance. The problem exhibits mathematical properties, e.g. strong convexity, that enable the utilization of dual splitting methods with analytic convergence bounds. In the first step, each PEV solves a local optimal program based on a broadcast price signal (the dual variables), and communicates their response to the aggregator. In the second step, the aggregator updates the price signal to achieve minimal load variance.

We propose three algorithms to compute this iterative process and analyze their convergence properties. This exposes computation and communication tradeoffs between the algorithms. (i) The gradient ascent method converges at a linear rate but requires an update from every agent at each iteration. (ii) The Incremental Stochastic Gradient Method

with constant step-size converges at a linear rate, needs an update from only one agent at each iteration but converges to an approximate solution. (iii) The Stochastic Incremental Method with decreasing step-size converges to the optimal solution as $\frac{1}{k}$ and requires an update from only one agent at each iteration.

Finally, we show that congestion constraints can be added to this framework, and the accelerated projected gradient solves the corresponding problem with a $\frac{1}{k^2}$ convergence rate. In the last section we compare the proposed method against previous decentralized algorithms, and consider a rolling horizon extension to avoid discontinuities between finite horizons. We present California-oriented case studies using real-world data from V2G-Sim, and quantify the potential of PEVs to flatten net load.

REFERENCES

[1] D. B. Richardson, Electric vehicles and the electric grid:a review of modeling approaches, impacts, and renewable energy integration, Renewable Sustainable Energy Reviews 19 (2013) 247–254.

[2] W. Kempton, J. Tomić, Vehicle-to-grid power fundamentals: Calculating capacity and net revenue, Journal of power sources 144 (1) 268–279.

[3] A. Langton, N. Crisostomo, Vehicle-grid integration: A vision for zero-emission transportation interconnected throughout california's electricity system, Tech. rep., California Public Utilities Commission.

[4] D. Callaway, I. Hiskens, Achieving controllability of electric loads, Proceedings of the IEEE 99 (1) (2011) 184–199. doi:10.1109/JPROC.2010.2081652.

[5] K. Clement, E. Haesen, J. Driesen, Coordinated charging of multiple plug-in hybrid electric vehicles in residential distribution grids, in: Power Systems Conference and Exposition, 2009. PSCE '09. IEEE/PES, 2009, pp. 1–7. doi:10.1109/PSCE.2009.4839973.

[6] E. Sortomme, M. Hindi, S. MacPherson, S. Venkata, Coordinated charging of plug-in hybrid electric vehicles to minimize distribution system losses, IEEE Transactions on Smart Grid 2 (1) (2011) 198–205. doi:10.1109/TSG.2010.2090913.

[7] C. Le Floch, F. Di Meglio, S. Moura, Optimal charging of vehicle-to-grid fleets via pde aggregation techniques, American Control Conference.

[8] P. Richardson, D. Flynn, A. Keane, Local versus centralized charging strategies for electric vehicles in low voltage distribution systems, Smart Grid, IEEE Transactions on 3 (2) (2012) 1020–1028. doi:10.1109/TSG.2012.2185523.

[9] Z. Ma, D. S. Callaway, I. A. Hiskens, Decentralized charging control of large populations of plug-in electric vehicles, IEEE Transactions on Control Systems Technology 21 (1) (2013) 67–78.

[10] L. Gan, U. Topcu, S. H. Low, Optimal decentralized protocol for electric vehicle charging, IEEE Transactions on Power Systems 28 (2) (2013) 940–951.

[11] Z. Tan, P. Yang, A. Nehorai, An optimal and distributed demand response strategy with electric vehicles in the smart grid, IEEE Transactions on Smart Grid 5 (2) (2014) 861–869. doi:10.1109/TSG.2013.2291330.

[12] J. Rivera, P. Wolfrum, S. Hirche, C. Goebel, H.-A. Jacobsen, Alternating direction method of multipliers for decentralized electric vehicle charging control, in: 2013 IEEE 52nd Annual Conference on Decision and Control (CDC), 2013, pp. 6960–6965. doi:10.1109/CDC.2013.6760992.

[13] S. Vagropoulos, A. Bakirtzis, Optimal bidding strategy for electric vehicle aggregators in electricity markets, Power Systems, IEEE Transactions on 28 (4) (2013) 4031–4041. doi:10.1109/TPWRS.2013.2274673.

[14] M. Gonzalez Vaya, G. Andersson, Optimal bidding strategy of a plug-in electric vehicle aggregator in day-ahead electricity markets under uncertainty, Power Systems, IEEE Transactions on 30 (5) (2015) 2375–2385. doi:10.1109/TPWRS.2014.2363159.

[15] R. Bessa, M. Matos, F. Soares, J. Lopes, Optimized bidding of a ev aggregation agent in the electricity market, Smart Grid, IEEE Transactions on 3 (1) (2012) 443–452. doi:10.1109/TSG.2011.2159632.

[16] S. Shao, M. Pipattanasomporn, S. Rahman, Demand response as a load shaping tool in an intelligent grid with electric vehicles, Smart Grid, IEEE Transactions on 2 (4) (2011) 624–631.

[17] S. Vandael, N. Boucké, T. Holvoet, G. Deconinck, Decentralized demand side management of plug-in hybrid vehicles in a smart grid, in: Proceedings of the First International Workshop on Agent Technologies for Energy Systems (ATES 2010), 2010, pp. 67–74.

[18] N. Chen, C. W. Tan, T. Q. Quek, Electric vehicle charging in smart grid: Optimality and valley-filling algorithms, Selected Topics in Signal Processing, IEEE Journal of 8 (6) (2014) 1073–1083.

[19] O. Sundström, C. Binding, Flexible charging optimization for electric vehicles considering distribution grid constraints, Smart Grid, IEEE Transactions on 3 (1) (2012) 26–37.

[20] W.-J. Ma, V. Gupta, U. Topcu, On distributed charging control of electric vehicles with power network capacity constraints, in: American Control Conference (ACC), 2014, IEEE, 2014, pp. 4306–4311.

[21] W. J. Ma, V. Gupta, U. Topcu, Distributed charging control of electric vehicles using regret minimization, in: 2014 IEEE 53rd Annual Conference on Decision and Control (CDC), 2014, pp. 4917–4923. doi:10.1109/CDC.2014.7040157.

[22] L. Gan, U. Topcu, S. H. Low, Stochastic distributed protocol for electric vehicle charging with discrete charging rate, in: Power and Energy Society General Meeting, 2012 IEEE, IEEE, 2012, pp. 1–8.

[23] Y. He, B. Venkatesh, L. Guan, Optimal scheduling for charging and discharging of electric vehicles, IEEE Transactions on Smart Grid 3 (3) (2012) 1095–1105.

[24] S. Bansal, M. N. Zeilinger, C. J. Tomlin, Plug-and-play model predictive control for electric vehicle charging and voltage control in smart grids, in: 2014 IEEE 53rd Annual Conference on Decision and Control (CDC), IEEE, 2014, pp. 5894–5900.

[25] J. Hu, S. You, M. Lind, J. Ostergaard, Coordinated charging of electric vehicles for congestion prevention in the distribution grid, IEEE Transactions on Smart Grid 5 (2) (2014) 703–711. doi:10.1109/TSG.2013.2279007.

[26] CAISO. What the duck curve tells us about managing a green grid [online].

[27] S. J. Moura, J. L. Stein, H. K. Fathy, Battery-health conscious power management in plug-in hybrid electric vehicles via electrochemical modeling and stochastic control, IEEE Transactions on Control Systems Technology 21 (3) (2013) 679–694.

[28] E. G. Brown, Zev action plan, Tech. rep. (February 2013).

[29] A. Blake, P. Kohli, C. Rother, Markov random fields for vision and image processing, Mit Press, 2011.

[30] S. Sra, S. Nowozin, S. J. Wright, Optimization for machine learning, Mit Press, 2012.

[31] P. L. Combettes, J.-C. Pesquet, Proximal splitting methods in signal processing, in: Fixed-point algorithms for inverse problems in science and engineering, Springer, 2011, pp. 185–212.

[32] M. Zhu, S. Martínez, On distributed convex optimization under inequality and equality constraints, Automatic Control, IEEE Transactions on 57 (1) (2012) 151–164.

[33] T.-H. Chang, A. Nedic, A. Scaglione, Distributed constrained optimization by consensus-based primal-dual perturbation method, Automatic Control, IEEE Transactions on 59 (6) (2014) 1524–1538.

[34] S. Boyd, L. Vandenberghe, Convex optimization, Cambridge university press, 2004.

[35] D. P. Bertsekas, Nonlinear programming.

[36] A. Nemirovski, A. Juditsky, G. Lan, A. Shapiro, Robust stochastic approximation approach to stochastic programming, SIAM Journal on Optimization 19 (4) (2009) 1574–1609.

[37] S. Song, K. Chaudhuri, A. D. Sarwate, Stochastic gradient descent with differentially private updates, in: IEEE Global Conference on Signal and Information Processing, 2013.

[38] J. Taylor, A. Maitra, M. Alexander, D. Brooks, M. Duvall, Evaluations of plug-in electric vehicle distribution system impacts, in: Power and Energy Society General Meeting, 2010 IEEE, 2010, pp. 1–6. doi:10.1109/PES.2010.5589538.

[39] M. Kintner-Meyer, K. Schneider, R. Pratt, Impacts assessment of plug-in hybrid vehicles on electric utilities and regional us power grids, part 1: Technical analysis, Pacific Northwest National Laboratory (2007) 1–20.

[40] Y. Nesterov, et al., Gradient methods for minimizing composite objective function (2007).

[41] V2g-sim [online].

[42] USDOT-FHWA, National Household Travel Survey, Tech. rep., U.S. Department of Transportation, http://nhts.ornl.gov/index.shtml (2009).

[43] S. Saxena, C. Le Floch, J. MacDonald, S. Moura, Quantifying ev battery end-of-life through analysis of travel needs with vehicle powertrain models, Journal of Power Sources.

[44] PGE. http://www.pge.com/en/mybusiness/rates/tvp/toupricing.page [online].